TRACKING THE MARTIAN MANTLE SIGNATURE IN OLIVINE-HOSTED MELT INCLUSIONS OF BASALTIC SHERGOTTITES YAMATO 980459 AND TISSINT.

T. J. Peters[1,2], J. I. Simon[2], J. H. Jones[3], T. Usui[1,4], R. Moriwaki[4], R. Economos[5], A. Schmitt[5], and K. McKeegan[5]. [1]Lunar and Planetary Institute, 3600 Bay Area Blvd., Houston, TX 77058 (peters@lpi.usra.edu); [2]Center for Isotope Cosmochemistry and Geochronology at ARES, NASA/JSC, Houston, TX 77058; [3]ARES, NASA/JSC, Houston, TX 77058; [4]Dept. of Earth and Planetary Sciences, Tokyo Institute of Technology. Tokyo 152-8551, Japan; [5]Dept of Earth and Space Sci, University of California Los Angeles, CA 90095, USA.

Introduction: The Martian shergottite meteorites are basaltic to lherzolitic igneous rocks that represent a period of relatively young mantle melting and volcanism, ~600-150 Ma (e.g. [1,2]). Their isotopic and elemental composition has provided important constraints on the accretion, evolution, structure and bulk composition of Mars.

Measurements of the radiogenic isotope and trace element concentrations of the shergottite meteorite suite have identified two end-members; (1) incompatible trace element enriched, with radiogenic Sr and negative ε^{143}Nd, and (2) incompatible trace-element depleted, with non-radiogenic Sr and positive ε^{143}Nd (e.g. [3-5]). The depleted component represents the shergottite martian mantle. The identity of the enriched component is subject to debate, and has been proposed to be either assimilated ancient martian crust [3] or from enriched domains in the martian mantle that may represent a late-stage magma ocean crystallization residue [4,5].

Olivine-phyric shergottites typically have the highest Mg# of the shergottite group and represent near-primitive melts having experienced minimal fractional crystallization or crystal accumulation [6]. Olivine-hosted melt inclusions (MI) in these shergottites represent the most chemically primitive components available to understand the nature of their source(s), melting processes in the martian mantle, and origin of enriched components.

We present trace element compositions of olivine hosted melt inclusions in two depleted olivine-phyric shergottites, Yamato 980459 (Y98) and Tissint (Fig. 1), and the mesostasis glass of Y98, using Secondary Ionization Mass Spectrometry (SIMS). We discuss our data in the context of understanding the nature and origin of the depleted martian mantle and the emergence of the enriched component.

Samples: Y98 and Tissint are olivine-phyric shergottites, displaying large olivine megacrysts set amongst a fine-grained groundmass. They represent martian volcanic lavas with a major element composition analogous to Fe-rich terrestrial picrites or komatiites.

Y98 has a fine-grained groundmass of olivine, pyroxene, chromite, and interstitial glassy mesostasis. The glassy mesostasis contains dendritic Fe-rich olivine and augite, and sulfide droplets [7], but unlike other olivine-phyric shergottites, Y98 contains no plagioclase/maskelynite or phosphate.

Tissint has a fine-grained groundmass of pyroxene and feldspathic glass (maskelynite), Ti-poor chromite, ilmenite, pyrrhotite and minor merrillite [8].

Both Y98 and Tissint are ideal candidates for constraining the composition of their primitive mantle source. They are the most magnesian shergottites known; Y98 Mg# = 66 [9], and Tissint Mg# = 60 [8]. They also have $^{87}Sr/^{86}Sr$ ratios lower than typical, terrestrial N-MORB and ε^{143}Nd values of +37 [10] and +42 [11,12] for Y98 and Tissint, respectively.

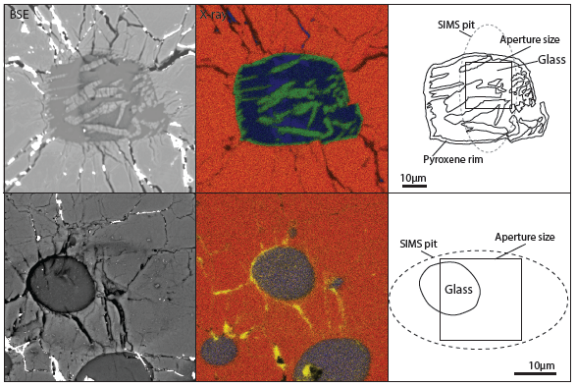

Figure. 1. Backscatter electron, X-ray, and sketch maps of representative melt inclusions in Tissint (Top) and Y98 (Bottom). Secondary minerals are absent in Y98. X-ray maps are Red = Mg, Yellow = Fe, Green = Ca, Blue = Al. Tissint pyroxene is $En_{28-36}Fs_{14-18}Wo_{50-56}$.

Analytical: Trace elements in glass phases were measured using the CAMECA ims-1270 SIMS at UCLA. The polished samples and standards were gold coated prior to analysis to avoid charging. We used a primary oxygen beam of 20 nA and 665 to 712 V energy filtering. Analyses were performed in mono-collection so that ion imaging could be employed. The data was reduced using measured ^{30}Si cps and the known SiO_2 wt% for the NIST 610 [13], and USGS BHVO-2 [14] and BCR-2 [15] glass standards, and the measured SiO_2 wt% for our glass locations.

Major element oxides for our glass phases and MI daughter phases were analyzed with the Cameca SX-100 EMPA at JSC. Analytical conditions were 15 kV, 20 nA, 30-60 second count times, and a 1 μm

beam. The measured element concentrations were adjusted to account for post-entrapment secondary olivine and pyroxene daughter crystallization.

Results: Chondrite-normalized REE profiles for both Y98 and Tissint MI's, and the Y98 mesostasis, parallel those of their bulk rock [8,9] (Fig. 2). We predict the MI profiles that plot below their bulk rock reflect a dilution of their trace element concentration with sputtering variable proportions of daughter phases or clipping of the olivine host (Fig. 1).

A flattening and upward inflection of La_N relative to Ce_N (Fig. 2), is a feature common to many of the depleted shergottites. Similar features in terrestrial primitive basalts indicate the addition of an external enriched component either to the source or assimilated prior to final crystallization. Our melt inclusion data supports the emergence of an enriched component to have been acquired at a time soon after melting and preceding extensive melt crystallization.

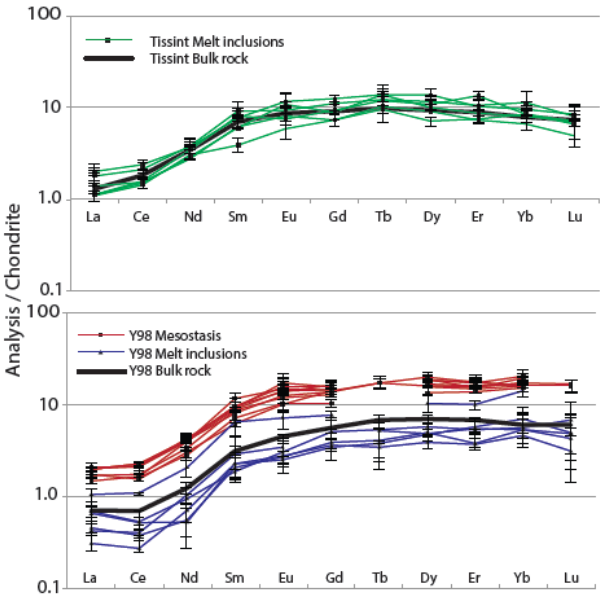

Figure. 2. Chondrite normalized REE plot for our analyses. Errors are 1σ.

Using compiled bulk rock shergottite geochemical data, we identify a range of incompatible element ratios that are insensitive to fractional crystallization and correlate with $\varepsilon^{143}Nd$ values. We use these element ratios to further track mixing between depleted and enriched components in our data.

To better understand the nature of these relationships and the origin of the shergottite sources, we discuss genetic links through variable partial melting of a fertile garnet lherzolite mantle for the early generation of the enriched and depleted shergottite reservoirs (Fig. 3).

The simplest model to account for the spread in shergottite isotopic and trace element composition (Fig. 3) is mixing between melts from an ancient melt depleted mantle and a trace-element enriched crust generated by small degrees of partial melting.

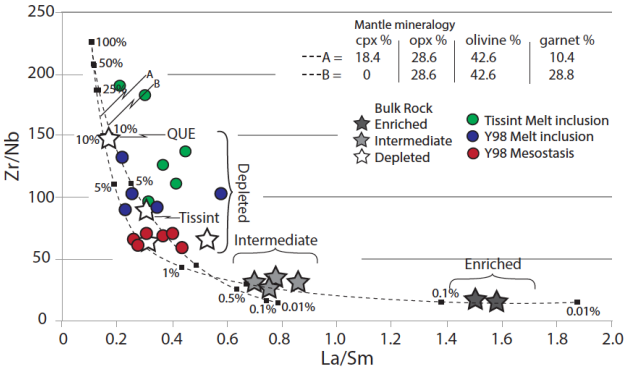

Figure. 3. Modeled partial melting trends of ancient martian mantle. Line A has mineral proportions from [16]. Line B has cpx suppressed and the proportion of garnet raised. %numbers represent the % of melting. The mantle source composition is calculated by assuming QUE94201 to be a 10% melt from this source.

We consider the enriched component to have resided near to the martian surface, at least close enough to interact with water that has exchanged with the martian atmosphere/hydrosphere [17]. This, however, requires the parental shergottite melts to have either left their respective source and remained closed to external input until reaching the enriched component, or the enriched component was introduced and mixed into the depleted source region prior to or during melting.

References:

[1] McSween H. Y. and Treiman A. H. (1998) *Rev Min Geo* 6, 6-01-6-54. [2] Nyquist L. E. et al. (2001) *Space Sci Rev* 96;105-164. [3] Jones J. H. (1989) *LPSC Proceedings* 19;465-474. [4] Borg L. E. et al. (1997) *GCA* 61;4915-4931. [5] Borg L. E. and Draper D. (2003) *Meteoritics & Planet. Sci.* 38;1713-1731. [6] Goodrich C. A. (2002) *MAPS* 37;B31-B34. [7] Usui T. et al. (2008) *GCA* 72;1711-1730. [8] Chennaoui Aoudjehane H. et al. (2012) *Science* 338;785-788. [9] Shirai N. and Ebihara M. (2004) *Antarctic Meteorite Research* 17;55. [10] Shih C. et al. (2005) *Antarctic Meteorite research* 18;46-65. [11] Grosshans T. E. et al. (2013) *LPS XLIV* Abstract #2872. [12] Brennecka G. A. et al. (2013) *LPS XLIV* Abstract #1786. [13] Rochell A. B. E. et al. (1997) *Geostandad Newslett* 21;101-114. [14] Wilson S. A. (1997) *USGS Open-File Report.* [15] Wilson S. A. (1997) *USGS Open-File Report* 98. [16] Blinova A. and Herd C. D. K. (2009) *GCA 73*;3471-3492. [17] Usui T. et al. (2012) *EPSL 357*;119-129.